

Dartmouth College Dartmouth Digital Commons

Open Dartmouth: Faculty Open Access Articles


4-13-2007

Membrane Association and Multimerization of TcpT, the Cognate ATPase Ortholog of the *Vibrio cholerae* Toxin-Coregulated-Pilus Biogenesis Apparatus

Shital A. Tripathi
Dartmouth College

Ronald K. Taylor
Dartmouth College

Follow this and additional works at: <https://digitalcommons.dartmouth.edu/facoa>

 Part of the [Bacteriology Commons](#), and the [Medical Microbiology Commons](#)

Recommended Citation

Tripathi, Shital A. and Taylor, Ronald K., "Membrane Association and Multimerization of TcpT, the Cognate ATPase Ortholog of the *Vibrio cholerae* Toxin-Coregulated-Pilus Biogenesis Apparatus" (2007). *Open Dartmouth: Faculty Open Access Articles*. 1092.
<https://digitalcommons.dartmouth.edu/facoa/1092>

This Article is brought to you for free and open access by Dartmouth Digital Commons. It has been accepted for inclusion in Open Dartmouth: Faculty Open Access Articles by an authorized administrator of Dartmouth Digital Commons. For more information, please contact dartmouthdigitalcommons@groups.dartmouth.edu.

Membrane Association and Multimerization of TcpT, the Cognate ATPase Ortholog of the *Vibrio cholerae* Toxin-Coregulated-Pilus Biogenesis Apparatus[∇]

Shital A. Tripathi and Ronald K. Taylor*

Department of Microbiology and Immunology, Dartmouth Medical School, Hanover, New Hampshire 03755

Received 2 January 2007/Accepted 3 April 2007

The toxin-coregulated pilus (TCP) is one of the major virulence factors of *Vibrio cholerae*. Biogenesis of this type 4 pilus (Tfp) requires a number of structural components encoded by the *tcp* operon. TcpT, the cognate putative ATPase, is required for TCP biogenesis and all TCP-mediated functions. We studied the stability and localization of TcpT in cells containing in-frame deletions in each of the *tcp* genes. TcpT was detectable in each of the biogenesis mutants except the $\Delta tcpT$ strain. TcpT was localized to the inner membrane (IM) in a TcpR-dependent manner. TcpR is a predicted bitopic inner membrane protein of the TCP biogenesis apparatus. Using metal affinity pull-down experiments, we demonstrated interaction between TcpT and TcpR. Using *Escherichia coli* as a heterologous system, we investigated direct interaction between TcpR and TcpT. We report that TcpR is sufficient for TcpT IM localization per se; however, stable IM localization of TcpT requires an additional *V. cholerae*-specific factor(s). A LexA-based two-hybrid system was utilized to define interaction domains of the two proteins. We demonstrate a strong interaction between the cytoplasmic domain of TcpR and the N-terminal 100 amino acid residues of TcpT. We also demonstrated the ability of the C-terminal domain of TcpT to multimerize.

Cholera, an acute gastrointestinal diarrheal disease, continues to threaten the world as a global public health problem, resulting in hundreds of thousands of cases per year (14). *Vibrio cholerae*, the causative agent of cholera, is a motile, gram-negative, comma-shaped bacterium that can be acquired by humans via consumption of contaminated food or water (22). Upon ingestion and survival of the gastric acid barrier, *V. cholerae* colonizes the upper intestine, manifesting pathogenesis by expressing various virulence factors. The toxin-coregulated pilus (TCP) is the major intestinal colonization factor of *V. cholerae*. TCP-deficient *V. cholerae* mutants are essentially completely defective in colonization of both humans and infant mice, the latter of which are used as a cholera model (17, 45, 47). TCP not only facilitates colonization directly, via mediating microcolony formation, but also mediates secretion of a soluble colonization factor, TcpF (24, 25). Upon colonization, *V. cholerae* secretes cholera toxin (CT), which deregulates ion transport by intestinal epithelial cells, leading to a massive loss of water and electrolytes, resulting in a characteristic “rice water stool” (22). TCP serves as the receptor for CTX Φ , which carries the CT genes (49). TCP provides a model for study of the biogenesis of type 4 pili (Tfp), enabling us to understand how microbes assemble a sophisticated macromolecular structure that participates in such various functions as colonization, extracellular secretion, and bacteriophage uptake. Based on the N-terminal sequence of the pilin and properties of the assembled filament, TCP shares the structural and functional characteristics of Tfp (44) and is classified into the subclass of

type 4b pili, which are often associated with intestinal infections, for example, the CFA/III pilus of enterotoxigenic *Escherichia coli* (ETEC), the CFC pilus of *Citrobacter rodentium*, and the bundle-forming pilus, BFP, of enteropathogenic *E. coli* (EPEC) (13, 29, 41, 46).

TCP biogenesis requires the products of at least 10 TCP-specific genes (*tcpA*, *tcpB*, *tcpQ*, *tcpC*, *tcpR*, *tcpD*, *tcpS*, *tcpT*, *tcpE*, and *tcpJ*), which are located, along with *tcpF*, in the *tcp* operon (23, 24, 27). In-frame deletion mutants of each of these *tcp* genes, though not *tcpF*, fail to assemble TCP (24). The *tcpF* gene encodes a colonization factor, TcpF, that is secreted via the TCP apparatus (24). One of the *tcp* genes, *tcpT*, encodes the cognate putative ATPase (20, 21). The presence of similar cognate ATPases, termed type II secretion ATPases, is a conserved feature found to be essential for Tfp biogenesis, and related type II secretion systems (T2SSs), in numerous gram-negative bacteria (for a review, see reference 37). TCP biogenesis has been shown to be dependent on TcpT (5). TcpT, like all Tfp and T2SS ATPases, does not contain any predicted transmembrane domain and is therefore hypothesized to peripherally associate to the TCP apparatus via direct interaction with an inner membrane (IM) protein component(s). TcpD, TcpE, TcpJ, and TcpR are the four *tcp*-encoded predicted IM proteins of the TCP apparatus. Topology prediction programs such as TMHMM (<http://www.cbs.dtu.dk/services/TMHMM/>) (43) indicate a bitopic topology for TcpD and TcpR and a polytopic topology for TcpJ and TcpE.

In this study, we provide evidence for the inner membrane localization of TcpT. TcpT was mislocalized to the cytoplasm in a *tcpR* deletion strain but not in *tcpD* or *tcpE* deletion mutants, indicating the necessity of TcpR for membrane tethering of TcpT. We have demonstrated interaction between TcpR and TcpT by using metal affinity pull-down experiments. This interaction was shown to be direct using TcpR-PhoA and

* Corresponding author. Mailing address: Dartmouth Medical School, Department of Microbiology and Immunology, HB7550, Hanover, NH 03755. Phone: (603) 650-1632. Fax: (603) 650-1318. E-mail: ronald.k.taylor@dartmouth.edu.

[∇] Published ahead of print on 13 April 2007.

TABLE 1. Strains and plasmids used in this study

Strain or plasmid	Relevant characteristics	Source or reference
<i>E. coli</i> strains		
SU101	JL1434 <i>lexA71::Tn5</i> (Def) <i>sulA211</i> Δ (<i>lacIPOZYA</i>)169/F' <i>lacI^qZΔM15::Tn9</i> (<i>op⁺/op⁺</i>)	10
SU202	<i>lexA71::Tn5</i> (Def) <i>sulA211</i> Δ <i>lacU</i> 169/F' <i>lacI^qZΔM15::Tn9</i> (<i>op⁴⁰⁸/op⁺</i>)	10
ST601	SU101(pSR662)	This study
ST602	SU202(pSR569)(pSR662)	This study
BL21(DE3)	F ⁻ <i>ompT</i> (<i>r_B⁻ m_B⁻</i>) (λ T7 RNA polymerase)	Lab collection
<i>V. cholerae</i> strains		
O395Sm	Classical Ogawa Sm ^r derivative	Lab collection
RT4493	O395Sm <i>tcpJ::Kan^r</i>	Lab collection
NB005	O395Sm Δ <i>tcpR</i> (pBADTOPO <i>TcpR</i> -6xHis Ap ^r)	Lab collection
MBN172	O395Sm Δ <i>tcpP</i>	30
Plasmids		
pSR569	Vector encoding the mutant LexA DBD sequence; Ap ^r	10
pSR662	Vector encoding the WT LexA DBD sequence; Tc ^r	10
pMA660-AraC	pSR662 derivative carrying the <i>lexA</i> DBD- <i>araC</i> fusion	19
pST03	pSR662 derivative carrying the LexA DBD-TcpT CTD (amino acids 251 to 503) fusion	This study
pST04	pSR662 derivative carrying the LexA DBD-full length TcpT fusion	This study
pST05	pSR662 derivative carrying the LexA DBD-TcpR cytoplasmic domain (amino acids 1 to 130) fusion	This study
pST06	pSR659 derivative carrying the mutant LexA-DBD-TcpT N-terminal domain (amino acids 1 to 100) fusion	This study
pST07	pSR659 derivative carrying the mutant LexA-DBD full-length TcpT fusion	This study
pST09	pSR662 derivative carrying the LexA DBD-TcpT N-terminal domain (amino acids 1 to 250) fusion	This study
pST10	pSR662 derivative carrying the LexA DBD-TcpR transmembrane domain (amino acids 131 to 151) fusion	This study
pST11	pSR659 derivative carrying the mutant LexA-DBD-TcpT-encoding (amino acids 101 to 503) fusion	This study
pST12	pBAD22 expressing full-length <i>tcpT</i> ; Ap ^r	This study
pPho7	P15A <i>oriV</i> MCS- <i>phoA</i> ; Ap ^r	15
pST13	pBAD33 expressing full-length <i>tcpR</i> fused to a 2.6-kb <i>phoA</i> fragment from pPho7; Cm ^r	This study

TcpT expressed in *E. coli*. The interactive domains of each were defined with a LexA-based bacterial heterologous-protein two-hybrid system. The ability to make homodimers was demonstrated for the C-terminal domain (CTD) of TcpT by using the LexA-based homologous-protein two-hybrid system.

MATERIALS AND METHODS

Bacterial strains, plasmids, culture conditions, and DNA manipulations. The strains and plasmids used in this study are listed in Table 1 except for the in-frame *tcp* deletion mutants, which have been reported previously (6, 24). *V. cholerae* and *E. coli* strains were maintained at -70°C in LB medium containing 30% (vol/vol) glycerol. *E. coli* cultures were grown in LB broth with a starting pH of 7.0 at 37°C for 12 to 16 h. In order to express TCP, *V. cholerae* strains were grown at 30°C in LB broth with a starting pH of 6.5 for 12 to 16 h. Antibiotics, when necessary, were used at the following concentrations: ampicillin (Ap), 100 $\mu\text{g}/\text{ml}$; chloramphenicol (Cm), 15 $\mu\text{g}/\text{ml}$; tetracycline (Tc), 15 $\mu\text{g}/\text{ml}$; streptomycin (Sm), 100 $\mu\text{g}/\text{ml}$. When required, IPTG (isopropyl- β -D-thiogalactopyranoside) was added to LB broth to 1 mM and arabinose was added to the growth media at concentrations ranging from 0.02% to 0.1%. All DNA manipulations were performed by standard molecular and genetic techniques (3, 26).

Subcellular fractionation. To prepare whole-cell extracts, cultures grown for 12 to 16 h were centrifuged and cells were resuspended in $2\times$ sodium dodecyl sulfate-polyacrylamide gel electrophoresis (SDS-PAGE) buffer with or without 2-mercaptoethanol and bromophenol blue (the latter to be used for protein estimation) and were boiled for 10 min. For membrane fractionation, a modification of a protocol based on differential solubility of membrane proteins in detergent sodium-lauryl sarcosinate (Sarkosyl) was utilized (6, 12). Briefly, 3 ml of culture grown for 12 to 16 h was harvested to fractionate periplasm and spheroplasts, and the latter were lysed by French pressure cell as described previously (6). After removal of unbroken spheroplasts by low-speed ($10,000\times g$ for 10 min) centrifugation, the clear lysate was centrifuged for 1 h at $100,000\times g$ at 4°C to separate soluble cytoplasm from insoluble total membrane fraction. The insoluble membrane fraction was resuspended in 1 ml of 10 mM Tris-Cl-100

mM NaCl (pH 8.0) containing 2.5% Sarkosyl, followed by a 30-min incubation on a platform rocker at room temperature. The insoluble outer membrane (OM) proteins were separated from the soluble IM proteins by ultracentrifugation at $200,000\times g$ for 1 h at 12°C . Pellets containing OM fractions were resuspended in 200 μl of 10 mM Tris-Cl (pH 8.0).

The purity of subcellular fractions was determined with immunoblotting and enzyme assays for known localization markers, as follows. EpsL and TcpC immunoblots were used as IM and OM localization markers, respectively (6, 38). As a cytoplasmic marker, glucose-6-phosphate dehydrogenase (G6PDH) activity was assayed (18). G6PDH substrate vials containing glucose-6-phosphate along with the cofactors NADP, PMS, and 2,6-dichlorophenol indophenol (DCP-IP) (Sigma) were reconstituted with 0.3 M Tris-Cl (pH 8.0) just prior to use, as recommended by the manufacturer. One milliliter of a 1:2 dilution of cytoplasmic fraction or 1 ml of IM fraction was added to a 4.5-ml cuvette containing the reconstituted substrate, immediately followed by an overlay of 2 ml of mineral oil. The decrease in the optical density at 600 nm (OD_{600}) was measured at 1-min intervals for 5 min to monitor the reduction of blue-colored DCP-IP to a colorless form (2). Specific activity was calculated as nanomoles of DCP-IP reduced per minute per milligram of total protein.

SDS-PAGE and immunoblot analysis. Protein concentrations of whole-cell extracts and subcellular fractions were determined with a BCA Protein Assay kit (Pierce). Samples containing equal amounts of total protein were resolved by 12.5% SDS-PAGE. Proteins were transferred to nitrocellulose membranes and probed individually with polyclonal antipeptide or monoclonal antibodies. Reactive bands were visualized with ECL detection reagents (Amersham Pharmacia).

Metal affinity chromatography. Cells were grown overnight under TCP-expressing conditions with or without the addition of 0.2% arabinose to induce expression of *TcpR*-6xHis. Cells were harvested and resuspended in extraction buffer (50 mM sodium phosphate-300 mM sodium chloride, pH 7.0) containing 1% vol/vol Triton X-100, 20 mM MgCl_2 , and DNase added to a final concentration of 20 $\mu\text{g}/\text{ml}$. The cells were broken by three passages through a French pressure cell at $8,000\text{ lb}/\text{in}^2$. Unbroken cells were removed by low-speed centrifugation. The lysates were incubated on a platform rocker at room temperature for 30 min. The clear lysates were mixed at a 1:1 ratio with TALON metal affinity

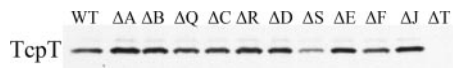


FIG. 1. Steady-state levels of TcpT in each of the TCP biogenesis mutants. Whole-cell extracts from *V. cholerae* WT and each indicated in-frame TCP biogenesis mutant were normalized for total protein and separated by SDS-PAGE, followed by immunoblotting with anti-TcpT antibody.

resin (Clontech) and allowed to mix on a rotating shaker for 1 h at 4°C. The protein purification protocol specified by the manufacturer was followed. The elution fraction was obtained with an extraction buffer containing 150 mM imidazole.

β-Galactosidase assay. For LexA-based homodimerization/heterodimerization experiments, expression of *sulA::lacZ* fusions was assayed from *E. coli* cultures grown at 37°C in LB, pH 7.0, containing 1 mM IPTG to an OD₆₀₀ of approximately 0.8 (10). β-Galactosidase activity was expressed as Miller units (28).

Protein localization prediction. The TMHMM program (<http://www.cbs.dtu.dk/services/TMHMM/>) (43) was used to predict the transmembrane helix topologies of TcpR, TcpD, TcpJ, and TcpE.

RESULTS

TcpT is detectable in all of the individual TCP biogenesis mutants except the ΔtcpT strain. The stability of the cognate ATPases of some Tfp systems and those of T2SSs have been shown to be affected by the absence of one or more accessory protein components of the cognate systems (4, 32, 36, 40). These reports led us to investigate the steady-state levels of TcpT in in-frame deletion mutants of each of the *tcp* genes. We observed similar abundances of TcpT in all of the IM *tcp* biogenesis mutants, i.e., in the Δ*tcpR*, Δ*tcpD*, Δ*tcpE*, and Δ*tcpJ* strains, compared to the wild-type (WT) strain (Fig. 1). However, we repeatedly noticed a decrease in the detectable amount of TcpT in a Δ*tcpS* strain and a slight increase in the detectable amount of TcpT in a Δ*tcpA* strain, as seen in Fig. 1. We did not observe any reproducibly significant difference in steady-state levels of TcpT in any of the other biogenesis mutants. The detectable levels of TcpT in all of the TCP biogenesis mutants, including the Δ*tcpS* strain, provided us the opportunity to determine the cellular localization of TcpT in each of the *tcp* biogenesis mutants.

TcpT is localized to the IM of WT *V. cholerae* but is mislocalized to the cytoplasm in a Δ*tcpR* strain. A previous model of TCP biogenesis (27) proposed that TcpT was localized to the IM via TcpE; however, this had not been examined experimentally. To test this model, we used subcellular fractionation to first demonstrate that the majority of TcpT is in fact localized to the IM in WT *V. cholerae* (Fig. 2A). The subcellular fractionation protocol was able to provide fairly pure fractions, as shown by the controls in Fig. 2A. TcpT was localized to the IM in each of the IM TCP biogenesis mutants except for the Δ*tcpR* strain, in which it was found to be almost entirely in the cytoplasm (Fig. 2B). Therefore, TcpR appears to be the major component that tethers TcpT to the IM. Complementation of the Δ*tcpR* strain using an arabinose-inducible p*TcpR*-6xHis construct restored IM localization of TcpT, as shown in Fig. 2C. Expression of this *TcpR*-6xHis construct in the Δ*tcpR* strain partially restored the WT TCP-associated phenotypes, such as autoagglutination, CTXΦ transduction, and TcpF se-

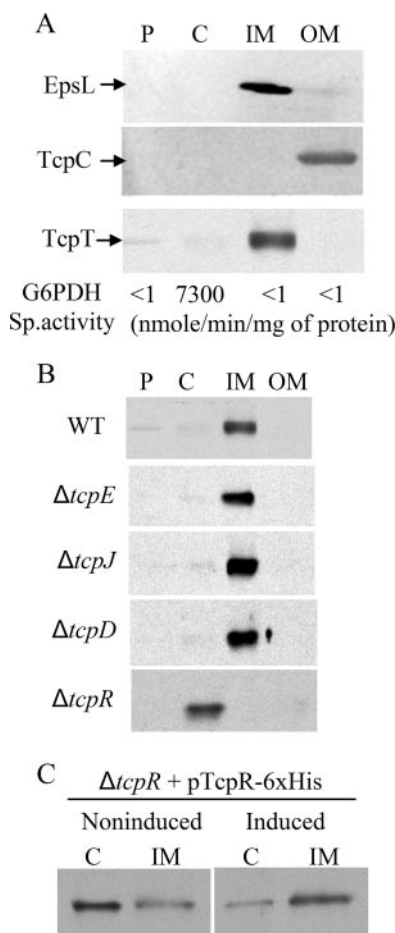


FIG. 2. TcpT localizes to the IM in a TcpR-dependent manner. (A) Perioplasmic (P), cytoplasmic (C), IM, and OM fractions from WT *V. cholerae* probed with fractionation control anti-EpsL (IM marker), anti-TcpC (OM marker), and anti-TcpT antibodies. The specific activity of G6PDH, a cytoplasmic marker, is indicated below each fraction. (B) Perioplasmic (P), cytoplasmic (C), IM, and OM fractions from WT and IM TCP biogenesis mutants probed with anti-TcpT antibody. (C) Cytoplasmic (C) and IM fractions of a *tcpR* deletion mutant complemented with p*TcpR*-6xHis grown under inducing and noninducing conditions and probed with anti-TcpT antibody.

cretion, indicating that His-tagged *TcpR* is functional (data not shown).

Steady-state levels of TcpT are higher in a Δ*tcpA* strain than in the WT strain. As shown in Fig. 1, there appeared to be a greater amount of TcpT detected in a Δ*tcpA* (pilin-negative) strain than in the WT. In order to determine if this was due to an overall increase in the steady-state level of membrane-bound TcpT or if it was also accompanied by mislocalization of TcpT, we performed a quantitative Western blot analysis of the cytoplasmic and IM fractions of a Δ*tcpA* strain for comparison with the fractionation profile of a WT strain. As shown in Fig. 3, the overall level of TcpT is greater in the Δ*tcpA* strain. Although more TcpT could be detected in the cytoplasmic fraction of the most-concentrated Δ*tcpA* lane, the overall ratio between the IM and cytoplasmic forms did not appear to be significantly altered. The levels of other TCP biogenesis components that have been examined previously were found to be

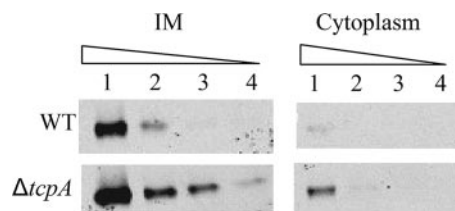


FIG. 3. Quantitative immunoblot analysis showing an overall increase in steady-state levels of TcpT in the $\Delta tcpA$ (pilin-negative) strain. IM and cytoplasmic fractions from WT and $\Delta tcpA$ strains were subjected to SDS-PAGE as a fivefold dilution series starting with 18 $\mu\text{g}/\text{ml}$ total protein and probed with anti-TcpT antibody.

normal in the $\Delta tcpA$ strain (6, 24). Moreover, there have not been any reports of strains or conditions wherein the steady-state level of any of the TCP biogenesis apparatus components is either increased or decreased due to a selective regulatory effect on gene expression. Therefore, it is likely that TcpT turnover is decreased specifically in the absence of pilin, as no other biogenesis mutants exhibit this effect.

TcpT interacts with TcpR. To determine if the role of TcpR in tethering TcpT to the IM is through interaction between the two proteins, we utilized metal affinity pull-down experiments to determine if TcpR-6xHis could pull down TcpT. Cell lysates were prepared from a $\Delta tcpR$ strain and the same strain complemented with pTcpR-6xHis grown under *tcp*-inducing conditions in the presence or absence of arabinose. Membrane proteins were solubilized with Triton X-100, and the resulting lysates were incubated with TALON metal affinity resin. The flowthrough and eluates from the metal affinity resin were subjected to immunoblot analysis (Fig. 4). The *tcpR* deletion strain served as a control to indicate that TcpR does not have any inherent affinity for binding to the metal affinity resin in the absence of TcpR. As seen in Fig. 4, upon induction, TcpR-6xHis was able to bind to the metal affinity resin and fractionate with the eluate, as shown by the anti-His immunoblot. Moreover, TcpR-6xHis was able to pull down TcpT, as indicated by coelution of TcpT. These data suggest that TcpR and TcpT are able to interact with each other in either a direct or an indirect manner.

TcpR is sufficient to direct TcpT to the IM but cannot tether it in a stable form in the absence of additional components. To address the ability of full-length TcpT to interact with full-length TcpR in the absence of other TCP proteins, we utilized *E. coli* as a heterologous system and attempted to coexpress TcpR-6xHis and TcpT. Our aim was to investigate TcpR-dependent IM localization of TcpT in the absence of the rest of the TCP proteins. We used the same TcpR-6xHis construct that was used to complement the *tcpR* deletion strain. However, we found that the TcpR-6xHis protein was undetectable when expressed in *E. coli* grown at either 30°C or 37°C, indicating that TcpR might be stabilized or stably held in the IM by another *V. cholerae* protein(s) (Fig. 5A). Consistent with this idea, the *V. cholerae* $\Delta tcpR$ strain complemented with the TcpR-6xHis construct expressed detectable amounts of TcpR-6xHis when the cells were grown under *tcp*-inducing conditions (30°C) but not when the expression of the *tcp* operon was only partially expressed (37°C) (Fig. 5A). Finally, we used a *tcpP* deletion strain, which lacks a transcriptional activator of *toxT*

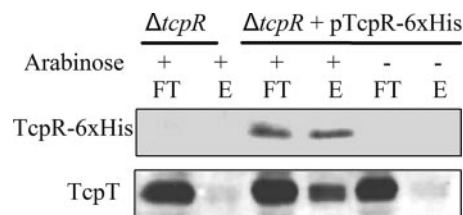


FIG. 4. TcpR and TcpT interaction is demonstrated by metal affinity chromatography. Whole-cell extracts from a *tcpR* deletion strain and *tcpR* complemented with pTcpR-6xHis grown under *tcpR::6xhis*-inducing (arabinose +) and noninducing (arabinose -) conditions were solubilized with 1% Triton X-100 and used for metal affinity chromatography as discussed in Materials and Methods. Flowthrough (FT) and elution (E) fractions were separated by SDS-PAGE and probed with anti-His and anti-TcpT antibodies.

expression (30). ToxT is the direct transcriptional activator of the *tcp* operon (16). We found that TcpR-6xHis could not be detected at either temperature in this strain (Fig. 5A).

One of the possible reasons for the observed instability of TcpR could be its unique predicted topology, with the IM domain at the extreme C terminus, leaving only one amino acid predicted to be exposed to the periplasm. Thus, it is likely that other IM proteins interact with TcpR to stabilize it in the IM. Interaction among the IM proteins of T2SSs via the IM domains has been reported previously with respect to the GSP (general secretion pathway) (which encompasses a T2SS) of *V. cholerae* (39). As we wanted to investigate whether TcpR on its own could direct TcpT to the IM, we attempted to stabilize TcpR by fusing it to PhoA at its C terminus. The *phoA* allele used to create this fusion lacks its own signal sequence. As shown in Fig. 5B, the fusion protein (corresponding to a size of about 49 kDa) was indeed stably localized to the IM of *E. coli* with or without coexpression of TcpT, as detected by subcellular fractionation followed by anti-PhoA immunoblotting. The fusion construct also produced alkaline phosphatase activity (data not shown), confirming the predicted topology of TcpR, i.e., the C terminus being exposed to the periplasm. As predicted, the expression of a *tcpT*-encoding construct alone resulted in localization of TcpT to the cytoplasm in *E. coli* (Fig. 5C). The coexpression of TcpT and TcpR-PhoA in *E. coli* resulted in the disappearance of the band corresponding to TcpT from the cytoplasmic fraction. Intriguingly, instead of concomitant localization of TcpT to the IM fraction, a complete disappearance of the band corresponding to the full-length TcpT protein was observed (Fig. 5C). Furthermore, we observed the appearance of a new band (designated TcpT*), which is most likely a degradation product of TcpT, localized to the IM fraction of these cells (Fig. 5C). Taken together, these results suggest that TcpR-PhoA is able to interact with TcpT in the absence of other TCP components and is able to direct tethering of TcpT to IM per se but not in a stable form. Furthermore, we recapitulated these results for *V. cholerae* by using the $\Delta tcpP$ strain. We observed that expression of *tcpT* in this strain resulted in stable TcpT with a localization defect (Fig. 5D). Coexpression of TcpT with TcpR-PhoA in the $\Delta tcpP$ strain resulted in the complete disappearance of TcpT from both the IM and cytoplasmic fractions. Consistent with the *E. coli* results, the majority of TcpR-PhoA was localized to the IM

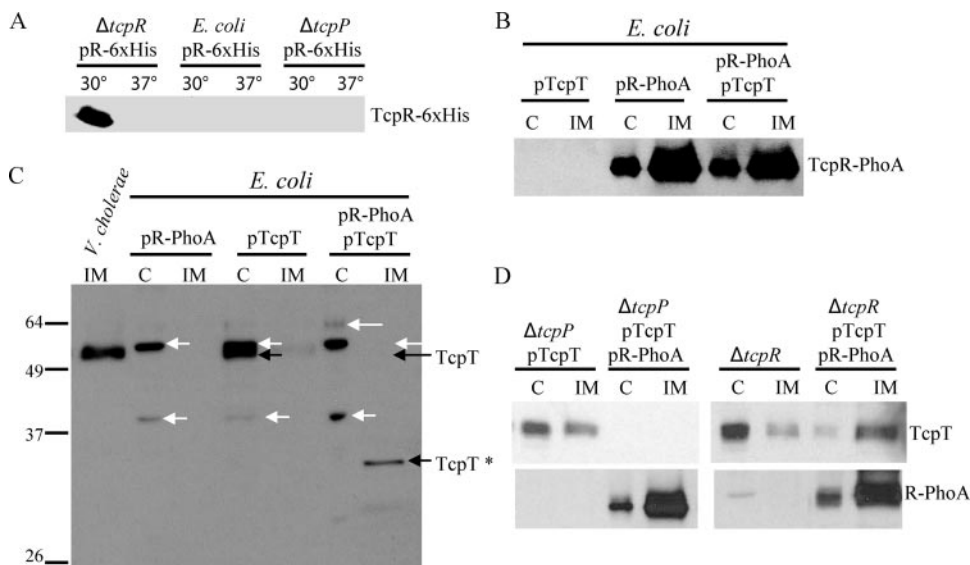


FIG. 5. TcpR is sufficient for IM localization of TcpT, but stable IM localization of TcpT and the stability of TcpR itself require additional *V. cholerae*-specific factors. (A) Whole-cell extracts of *V. cholerae* $\Delta tcpR$, *E. coli* BL21, or *V. cholerae* $\Delta tcpP$ carrying a TcpR-6xHis construct, grown in the presence of 0.02% arabinose at both 30°C (*tcp* expression ON in *V. cholerae*) and 37°C and separated by SDS-PAGE, followed by anti-His immunoblotting. (B) Cytoplasmic (C) and IM fractions from *E. coli* BL21 expressing the indicated combination of TcpR-PhoA and/or TcpT constructs were separated by SDS-PAGE, followed by anti-PhoA immunoblotting. (C) WT *V. cholerae* IM fraction (first lane only) and *E. coli* BL21 cytoplasmic (C) and IM fractions were separated by SDS-PAGE, followed by immunoblotting using anti-TcpT antibody. The black arrows indicate bands corresponding to either TcpT or a putative degradation product of TcpT (indicated as TcpT*), and the white arrows indicate nonspecific bands. (D) SDS-PAGE followed by immunoblotting of the cytoplasmic (C) and IM fractions of a *tcpP* deletion mutant and a *tcpR* deletion mutant expressing TcpT and/or TcpR-PhoA grown under TCP-inducing conditions and probed with anti-TcpT (top) and anti-PhoA antibody (bottom).

fraction in this strain (Fig. 5D, bottom). Conversely, expression of TcpR-PhoA was able to complement a $\Delta tcpR$ strain, as shown by nearly complete restoration of localization of TcpT to the IM (Fig. 5D) as well as by partial restoration of other functional TCP phenotypes (data not shown). Taken together, these results show that TcpR is sufficient to direct TcpT to the IM but that stable localization of TcpT to the IM and the stability of TcpR itself require other *V. cholerae*-specific factors, most likely other IM components of the TCP biogenesis apparatus.

The cytoplasmic N-terminal domain of TcpR interacts with the N-terminal domain of TcpT. TcpR is a relatively small protein, consisting of 151 amino acid residues. Localization and topology prediction programs such as TMHMM (43) predict a bitopic TcpR topology in which TcpR spans the IM a single time, with the N-terminal 130 residues residing in the cytoplasm and only the last C-terminal residue being exposed on the periplasmic side. Thus, we hypothesized that the cytoplasmic 130-amino-acid region of TcpR might include the domain that directly interacts with TcpT. Unlike TcpR, TcpT is a bigger protein, consisting of 503 amino acid residues. We performed a primary sequence alignment of TcpT with the cognate ATPases of similar systems, such as EpsE, of the T2SS of *V. cholerae*, and OutE, of the T2SS of *Erwinia chrysanthemi*, and found three distinct domains of the proteins with respect to sequence conservation. The first domain, the N-terminal 100-amino-acid domain, represents a region of weak alignment (5 to 6% identity and 12 to 16% similarity). This is followed by the middle, more-conserved region, from amino acid 101 to 350 (25 to 26% identity and 40 to 42% similarity), which includes the predicted conserved sequence of catalytic impor-

tance, and then the CTD, from residues 351 to 503, which exhibits an intermediate alignment (18 to 19% identity and 30 to 33% similarity). It has been shown that the cognate membrane protein association domains of EpsE and OutE are present within the N-terminal 100 amino acid residues, whereas the C-terminal region is involved in homodimerization (34, 37). To investigate the possibility of the first (N-terminal) 100 residues of TcpT interacting with the predicted cytoplasmic domain of TcpR, we created LexA fusion constructs of various domains of TcpR and TcpT for use in a bacterial two-hybrid protein system (10) (Fig. 6A). This system allows detection of heterodimeric interactions because (for example, in our case), the TcpR cytoplasmic fragment is fused to a WT LexA DNA binding domain (DBD) that recognizes a WT half-site and the TcpT fragment is fused to a LexA mutant DBD that recognizes a mutant half-site. The reporter *sulA::lacZ* carries a hybrid LexA binding site. One half-site is WT and the other is recognized only by the mutant LexA DBD (10). Plasmids encoding fusion proteins carrying different domains of TcpT and TcpR (Fig. 6A) were cotransformed into the *E. coli* SU202 strain carrying a *sulA::lacZ* reporter gene with the hybrid LexA binding site. The possible interactions were measured in terms of repression of *sulA::lacZ* expression (Fig. 6B). Each sample was also analyzed by immunoblotting with anti-LexA antibody to determine whether the hybrid constructs were all expressed at similar levels. As shown in Fig. 6B, the N-terminal 100-amino-acid-residue-containing domain of TcpT, in combination with the cytoplasmic domain of TcpR, resulted in almost 20-fold repression of *sulA::lacZ* expression compared to the vector control and the control strains expressing either construct individually. The LexA fusion construct

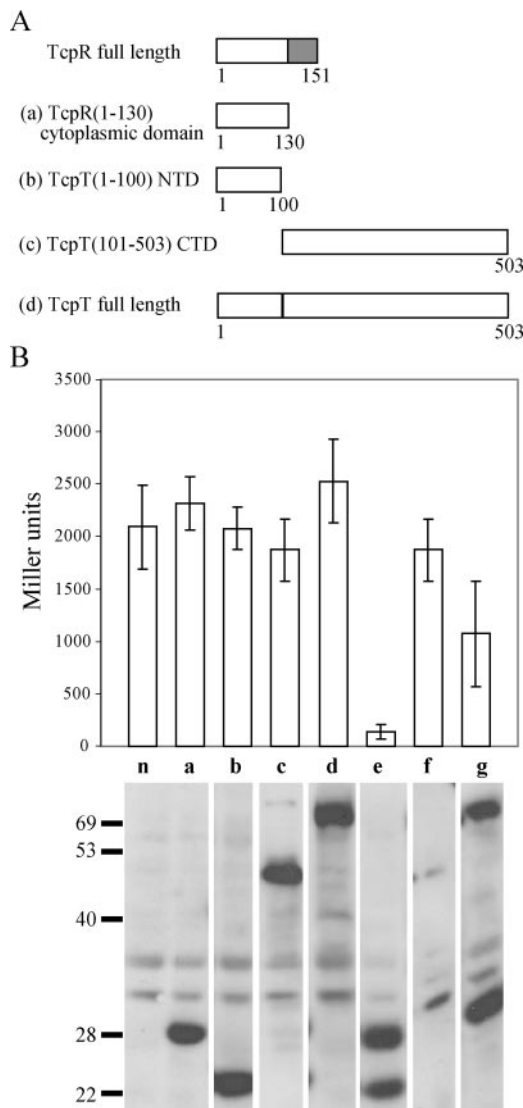


FIG. 6. The N terminus of TcpT interacts with the predicted cytoplasmic domain of TcpR, as demonstrated by a LexA-based two-hybrid protein system. (A) Representation of various TcpT and TcpR constructs fused to the N terminus of LexA. The letter designation for each of the constructs corresponds to the data shown in panel B. The grey box represents the transmembrane domain of TcpR. (B) *E. coli* SU202 carrying various constructs was grown to an OD_{600} of approximately 0.8 in the presence of 1 mM IPTG, and expression of *sulA::lacZ* was measured by β -galactosidase assays. n, negative control, i.e., coexpression of empty vectors; a, TcpR (amino acids 1 to 130) cytoplasmic domain; b, TcpT (amino acids 1 to 100) N-terminal domain; c, TcpT (amino acids 101 to 503) CTD; d, TcpT full-length protein; e, coexpression of a and b; f, coexpression of a and c; g, coexpression of a and d. The stability of each of the fusion proteins was detected by anti-LexA immunoblotting, and a composite that includes one representative sample selected for each strain (the strains were analyzed in triplicates) is shown at the base of the graph for each of the respective strains.

carrying the remainder of TcpT (residues 101 to 503), when coexpressed with the cytoplasmic domain of the TcpR fusion protein, failed to repress *sulA::lacZ* (Fig. 6B) but resulted in destabilization of both of the fusion proteins, which were otherwise stable when not coexpressed (see the LexA immunoblot

in Fig. 6B to compare sample panels a and c with f). This result indicates that the TcpT CTD (amino acids 101 to 503) may contain another TcpR interaction site that could result in a nonproductive interaction, i.e., leading to instability of the fusion proteins. Coexpression of the TcpR cytoplasmic domain fusion protein with full-length TcpT failed to exhibit a strong interaction, as indicated by only a twofold repression of *sulA::lacZ* expression (Fig. 6B). Similar results for a full-length ATPase fusion construct interaction with its respective IM protein fusion construct in a yeast two-hybrid system have been reported for OutE (34). The inability of the full-length protein to exhibit a strong positive interaction with the cytoplasmic domain of TcpR could be due to the fact that TcpT also exhibits characteristic homodimerization involving the CTD of the protein (see below), which may interfere with the heterodimerization assay. Alternatively, it is possible that the full-length TcpT requires the IM domain of TcpR in order to interact with TcpR.

The C terminus of TcpT can mediate homodimerization. Using a LexA-based homologous two-hybrid system (10), we investigated the domains involved in possible multimerization of TcpT. As shown in the Fig. 7A, approximately half of the TcpT protein from either the C terminus or the N terminus was fused with the N terminus of the WT LexA DBD by using pSR662 (10). Possible homodimerization was quantified in terms of repression of *lacZ* expression in *E. coli* SU101 carrying a *sulA::lacZ* reporter gene containing two WT LexA half-sites in the promoter region. As shown in Fig. 7B, the fusion protein containing the C-terminal half, but not the N-terminal half, of TcpT exhibited a strong repression of *sulA::lacZ*, indicating homodimerization, similar to that seen with the AraC fusion construct used as a positive control. However, full-length TcpT failed to exhibit *sulA::lacZ* repression, similar to the results reported previously for OutE (34). It is not clear why full-length TcpT would not mediate homodimerization and thus repression of *sulA::lacZ* as well as the CTD alone. One speculation is that the bulkier size of the full-length protein might cause a steric hindrance between two LexA monomers that interferes with DNA binding, a possible limitation of the LexA-based hybrid protein system that has been discussed previously (10).

DISCUSSION

In the present study, using biochemical and genetic approaches, we have investigated the stability, localization, and protein-protein interaction of TcpT with respect to the TCP biogenesis apparatus components. We present evidence for IM localization of TcpT in WT *V. cholerae*. The fact that TcpT localizes to the IM in WT *V. cholerae* is consistent with previously reported IM localization of the cognate ATPases of other Tfp and T2SS complexes (4, 8, 32, 34, 40). We used a collection of in-frame *tcp* single-gene deletion mutants to investigate the requirement of the corresponding TCP components in tethering TcpT to the IM and found that TcpR was necessary for TcpT association with the IM. TcpR is a predicted bitopic IM protein that is a GspL homolog (33). Our results add to a common theme emerging from various studies showing IM localization of the cognate ATPase by a bitopic IM protein, GspL, of the IM platform of a T2SS or a Tfp (4, 8, 32, 35, 40).

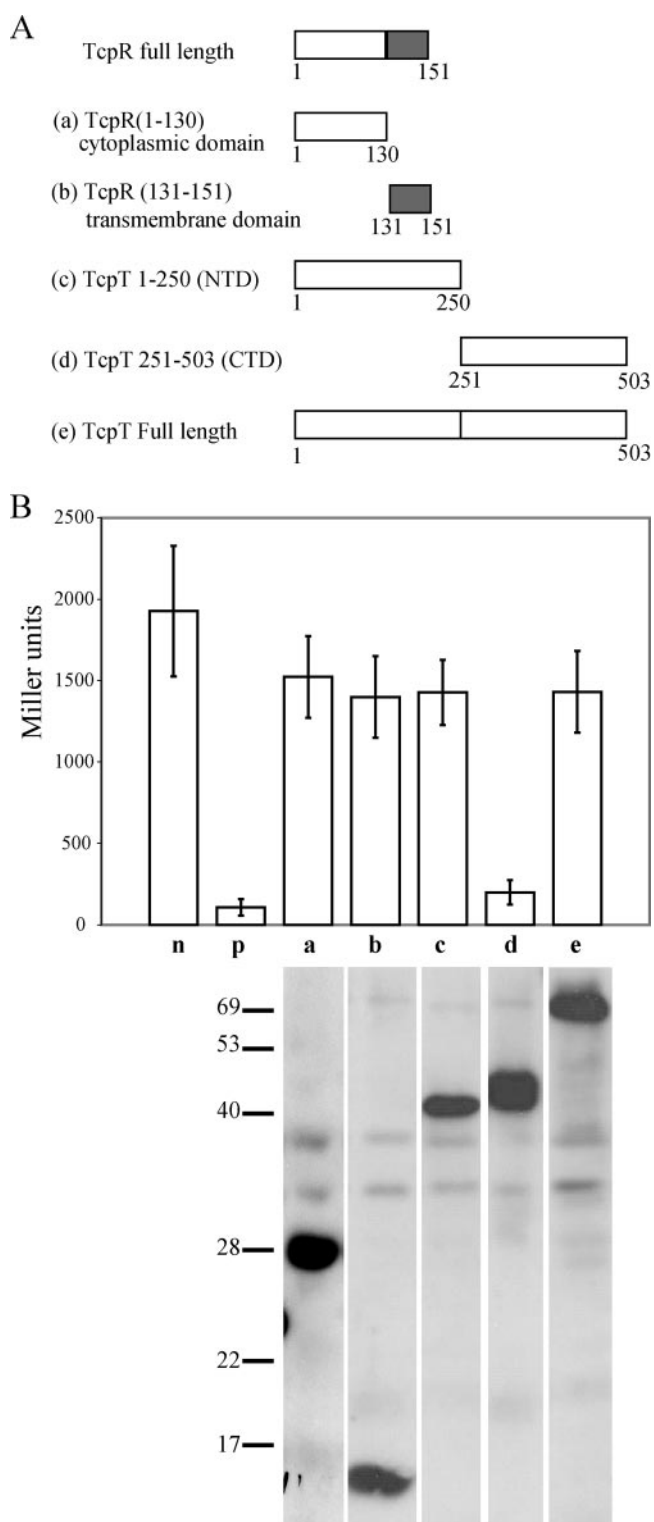


FIG. 7. The C terminus of TcpT can form multimers, as demonstrated by a LexA-based homologous protein two-hybrid protein system. (A) Representation of various TcpT and TcpR constructs fused to the N terminus of LexA. The letter designated for each of the constructs corresponds to the data shown in panel B. The grey boxes represent the transmembrane domain of TcpR. (B) Analysis of the ability of various TcpT and TcpR constructs to form homodimers. Strains of SU101 were grown to an OD_{600} of approximately 0.8 in the presence of 1 mM IPTG, and expression of *sulA::lacZ* was measured

In this study, we have demonstrated interaction between TcpT and TcpR by using metal affinity pull-down experiments. In order to investigate whether this interaction is direct or not, we coexpressed TcpR-PhoA and TcpT in the absence of other TCP proteins either in a heterologous system such as *E. coli* or in a $\Delta tcpP$ strain. In these cases, TcpR, by itself, directed TcpT to the membrane but in a manner that led to its degradation. Such conformational changes upon interaction between the ATPase and the cognate IM proteins of both a T2SS and a Tfp have been reported, such as the examples of the ATPases BfpD and EpsE becoming unstable when coexpressed with the cognate bitopic IM proteins BfpC and EpsL, respectively (1, 8).

The use of a LexA-based two-hybrid system that is designed to investigate heterodimerization among proteins allowed us to determine the regions of TcpT that are capable of interacting with the cytoplasmic domain of TcpR. We showed that the direct stable interaction between TcpR and TcpT involves the N-terminal portion (amino acids 1 to 100) of TcpT and the cytoplasmic domain of TcpR. This result is consistent with the evidence for other GspE-GspL cognate interactions in T2SSs (32, 34, 40). The second interaction between TcpT and TcpR seems to involve the CTD (amino acids 101 to 503) of TcpT and the cytoplasmic domain of TcpR. Although the LexA fusions containing these two regions of TcpT and TcpR did not exhibit a positive interaction, as indicated by the expression of *sulA::lacZ* reporter system, the coexpression of these fusion proteins resulted in instability of both, indicating a nonproductive or antagonistic interaction between these two regions of TcpT and TcpR. Therefore, in addition to the first N-terminal 100 residues, TcpT (amino acids 101 to 503) might contain a second site of TcpR interaction that could be a physiologically significant interaction. The former interaction might form a stable complex between TcpR and TcpT at the IM, whereas the latter (TcpT [amino acids 101 to 503]-TcpR) interaction might result in a conformational change in both of the proteins, which might mimic an active (ready for ATP hydrolysis) complex that needs to be stabilized by other TCP components. In the case of BFP, noted above, the reason for destabilization of BfpD upon coexpression with BfpC was shown to be due to mutual conformational changes in both proteins (8). The regions of BfpD interacting with BfpC are not yet mapped. Based on our results, we predict that a nonproductive interaction such as that reported here (TcpT [amino acids 101 to 503]-TcpR) might cause mutual conformational changes, resulting in destabilization of both BfpD and BfpC. Consistent with this notion, Abendroth et al. attempted to crystallize the EpsE ATPase bound to the cytoplasmic domain of the cognate IM protein EpsL and found that the full-length ATPase was

by β -galactosidase assays. n, negative control, i.e., empty vector; p, positive control AraC-LexA construct; a, TcpR cytoplasmic domain (amino acids 1 to 130); b, TcpR transmembrane domain (amino acids 131 to 151); c, TcpT N-terminal domain (amino acids 1 to 250); d, TcpT CTD (amino acids 251 to 503); e, TcpT full-length protein. The stability of each of the fusion proteins was detected by anti-LexA immunoblotting, and a composite that includes a representative sample for each strain (the strains were analyzed in triplicate) is shown at the base of the graph for each of the respective strains.

highly susceptible to proteolysis, resulting in a small stable fragment consisting of the N-terminal 1- to 88-amino-acid domain of the protein that could be cocrystallized with the cytoplasmic domain of EpsL (1). Based on our results and these reported studies, we predict that an additional GspL interaction site(s), besides the N-terminal 100 residues in the cognate ATPases of GSP (GspE), could indeed be a common feature of the interaction of the cognate ATPases with the cognate bitopic membrane proteins.

Using a LexA-based homodimerization system, we demonstrated the ability of the C terminus of TcpT to mediate homodimerization. Homodimerization has been reported for various GspE homologs of T2SSs (32, 34, 48). It is becoming clear that most of these cognate ATPases of T2SSs, as well as the homologs of Tfp, such as BfpD, are capable of forming homohexamers (7, 9, 37, 42). Homodimerizations of the TcpR homolog of the BFP IM platform, BfpC, and T2SS (GspL) have also been reported (8, 32, 34, 38). Using the LexA-based homodimerization system, we were unable to detect TcpR homodimerization mediated by either the cytoplasmic domain or the membrane domain of TcpR. However, these results could reflect limitations of the LexA-based homodimerization system to detect interactions among transmembrane proteins. Therefore, additional approaches will be needed to investigate the possible homodimerization of TcpR.

An interesting outcome of our study was the finding that, in the absence of pilin (in a *tcpA* deletion strain), the steady-state levels of TcpT increased with no gross mislocalization. To explain the relationship between the pilin monomer and TcpT turnover, one hypothesis is that there is a direct interaction between TcpT and the pilin (the substrate monomers) that induces a conformational change in TcpT, perhaps analogous to that seen for SecA and its substrates (11, 31). This TcpA-mediated TcpT conformational change might affect TcpT stability. Another possibility is that in the absence of TcpA, the conformational status of the TCP IM platform is different in such a way that the TcpR-mediated tethering of TcpT results in an increasingly stable conformation of TcpT, resulting in increased steady-state levels of TcpT in the $\Delta tcpA$ strain.

We observed decreased steady-state levels of TcpT in a *tcpS* deletion strain. This result is entirely consistent with the BFP system, in which the absence of the cognate periplasmic protein BfpU resulted in a decrease in the detection of the cognate ATPase, BfpD, compared to the WT EPEC strain (36).

The fact that twitching motility has not been observed under any experimental conditions for *V. cholerae* and that the *tcp* operon lacks a *pilT* (encoding an ATPase associated with retraction) ortholog and genes encoding more than one pseudo-pilin suggests that the TCP biogenesis apparatus structure and function might differ from those of the retractile Tfp elaborated by bacteria such as EPEC, *P. aeruginosa*, or *N. gonorrhoeae*. In agreement with this notion is the recent finding that Tfp gene clusters encoding the CFA/III pilus of ETEC and the CFC pilus of *Citrobacter rodentium* (29, 46) exhibit a greater resemblance to *tcp* in terms of the genetic organization of the respective operons. Furthermore, the primary sequences of the respective pilus apparatus proteins exhibited close analogy to the TCP proteins, indicating that TCP might represent a functional prototype of this sub-subclass of Tfp. Understanding the molecular interactions among TCP apparatus components and

their impact on the assembly and function of the TCP apparatus is therefore a key to studying these specialized macromolecular assemblies, which are elaborated by various pathogenic bacteria.

ACKNOWLEDGMENTS

We thank Maria Sandkvist for antibody directed against EpsL. This work was supported by National Institutes of Health grant AI25096 to R.K.T.

REFERENCES

1. Abendroth, J., P. Murphy, M. Sandkvist, A. M. Bagdasarian, and G. J. H. Wim. 2005. The X-ray structure of the type II secretion system complex formed by the N-terminal domain of EpsE and the cytoplasmic domain of EpsL of *Vibrio cholerae*. *J. Mol. Biol.* **348**:845–855.
2. Aiuchi, T., S. Nakajo, and K. Nakaya. 2004. Reducing activity of colloidal platinum nanoparticles for hydrogen peroxide, 2,2-DPPR and 2,6-DCP-IP. *Biol. Pharm. Bull.* **27**:736–738.
3. Ausubel, F. M., R. Brent, R. E. Kingston, D. D. Moore, J. G. Seidman, J. A. Smith, and K. Struhl. 1987. Current protocols in molecular biology. Greene Publishing Associates and John Wiley & Sons, New York, NY.
4. Ball, G., V. Chapon-Herve, S. Bleves, G. Michel, and M. Bally. 1999. Assembly of XcpR in the cytoplasmic membrane is required for extracellular protein secretion in *Pseudomonas aeruginosa*. *J. Bacteriol.* **181**:382–388.
5. Bose, N., S. M. Payne, and R. K. Taylor. 2002. Type 4 pilus biogenesis and type II-mediated protein secretion by *Vibrio cholerae* occur independently of the TonB-facilitated proton motive force. *J. Bacteriol.* **184**:2305–2309.
6. Bose, N., and R. K. Taylor. 2005. Identification of a TcpC-TcpQ outer membrane complex involved in the biogenesis of the toxin-coregulated pilus of *Vibrio cholerae*. *J. Bacteriol.* **187**:2225–2232.
7. Camberg, J. L., and M. Sandkvist. 2005. Molecular analysis of the *Vibrio cholerae* type II secretion ATPase EpsE. *J. Bacteriol.* **187**:249–256.
8. Crowther, L. J., R. P. Anantha, and M. S. Donnenberg. 2004. The inner membrane subassembly of the enteropathogenic *Escherichia coli* bundle-forming pilus machine. *Mol. Microbiol.* **52**:67–79.
9. Crowther, L. J., A. Yamagata, L. Craig, J. A. Tainer, and M. S. Donnenberg. 2005. The ATPase activity of BfpD is greatly enhanced by zinc and allosteric interactions with other Bfp proteins. *J. Biol. Chem.* **280**:24839–24848.
10. Daines, D. A., and R. P. Silver. 2000. Evidence for multimerization of Neu proteins involved in polysialic acid synthesis in *Escherichia coli* K1 using improved LexA-based vectors. *J. Bacteriol.* **182**:5267–5270.
11. Ding, H., I. Mukerji, and D. Oliver. 2001. Lipid and signal peptide-induced conformational changes within the C-domain of *Escherichia coli* SecA protein. *Biochemistry* **40**:1835–1843.
12. Fillip, C., G. Fletcher, J. L. Wulff, and C. F. Earhart. 1973. Solubilization of the cytoplasmic membrane of *Escherichia coli* by the ionic detergent sodium lauryl sarcosinate. *J. Bacteriol.* **115**:717–722.
13. Giron, J. A., A. S. Ho, and G. K. Schoolnik. 1991. An inducible bundle-forming pilus of enteropathogenic *Escherichia coli*. *Science* **254**:710–713.
14. Griffith, D. C., L. A. Kelly-Hope, and M. A. Miller. 2006. Review of reported cholera outbreaks worldwide, 1995–2005. *Am. J. Trop. Med. Hyg.* **75**:973–977.
15. Gutierrez, C., and J. C. Devedjian. 1989. A plasmid facilitating in vitro construction of *phoA* gene fusions in *Escherichia coli*. *Nucleic Acids Res.* **17**:3999.
16. Hase, C. C., and J. J. Mekalanos. 1998. TcpP protein is a positive regulator of virulence gene expression in *Vibrio cholerae*. *Proc. Natl. Acad. Sci. USA* **95**:730–734.
17. Herrington, D. A., R. H. Hall, G. Losonsky, J. J. Mekalanos, R. K. Taylor, and M. M. Levin. 1988. Toxin, toxin co-regulated pili and the *toxR* regulon are essential for *Vibrio cholerae* colonization in humans. *J. Exp. Med.* **168**:1487–1492.
18. Hillar, A., L. Van Caesele, and P. C. Loewen. 1999. Intracellular location of catalase-peroxidase hydroperoxidase I of *Escherichia coli*. *FEMS Microbiol. Lett.* **170**:307–312.
19. Ibarra, J. A., M. I. Villalba, and J. L. Puente. 2003. Identification of the DNA binding sites of PerA, the transcriptional activator of the *bfp* and *per* operons in enteropathogenic *Escherichia coli*. *J. Bacteriol.* **185**:2835–2847.
20. Iredell, J. R., and P. A. Manning. 1994. The toxin-co-regulated pilus of *Vibrio cholerae* O1: a model for type 4 pilus biogenesis? *Trends Microbiol.* **2**:187–192.
21. Iredell, J. R., and P. A. Manning. 1997. Translocation failure in a type-4 pilin operon: *rfb* and *tcpT* mutants in *Vibrio cholerae*. *Gene* **192**:71–77.
22. Kaper, J. B., J. G. Morris, and M. M. Levin. 1995. Cholera. *Clin. Microbiol. Rev.* **8**:48–86.
23. Kaufman, M. R., C. E. Shaw, I. D. Jones, and R. K. Taylor. 1993. Biogenesis and regulation of the *Vibrio cholerae* toxin-coregulated pilus: analogies to other virulence factor secretory systems. *Gene* **126**:43–49.

24. Kirn, T. J., N. Bose, and R. K. Taylor. 2003. Secretion of a soluble colonization factor by the TCP type 4 pilus biogenesis pathway in *Vibrio cholerae*. *Mol. Microbiol.* **49**:81–92.
25. Kirn, T. J., M. J. Lafferty, C. M. P. Sandoe, and R. K. Taylor. 2000. Delineation of pilin domains required for bacterial association into microcolonies and intestinal colonization by *Vibrio cholerae*. *Mol. Microbiol.* **35**:896–910.
26. Maniatis, T., E. F. Fritsch, and J. Sambrook. 1982. Molecular cloning: a laboratory manual. Cold Spring Harbor Laboratory Press, Cold Spring Harbor, NY.
27. Manning, P. A. 1997. The *tcp* gene cluster of *Vibrio cholerae*. *Gene* **192**:63–70.
28. Miller, J. H. 1972. Experiments in molecular genetics. Cold Spring Harbor Laboratory Press, Cold Spring Harbor, NY.
29. Mundy, R., D. Pickard, R. K. Wilson, C. P. Simmons, G. Dougan, and G. Frankel. 2003. Identification of a novel type IV pilus gene cluster required for gastrointestinal colonization of *Citrobacter rodentium*. *Mol. Microbiol.* **48**:795–809.
30. Nye, M. B., J. D. Pfau, K. Skorupski, and R. K. Taylor. 2000. *Vibrio cholerae* H-NS silences virulence gene expression at multiple steps in the ToxR regulatory cascade. *J. Bacteriol.* **182**:4295–4303.
31. Papanikou, E., S. Karamanou, C. Baud, M. Frank, G. Sianidis, D. Keramisanou, C. G. Kalodimos, A. Kuhn, and A. Economou. 2005. Identification of the preprotein binding domain of SecA. *J. Biol. Chem.* **280**:43209–43217.
32. Possot, O. M., G. Vignon, N. Bomchil, F. Ebel, and A. P. Pugsley. 2000. Multiple interactions between pullulanase secretion components involved in stabilization and cytoplasmic membrane association of PulE. *J. Bacteriol.* **182**:2142–2152.
33. Pugsley, A. P. 1993. The complete general secretory pathway in gram-negative bacteria. *Microbiol. Rev.* **57**:50–108.
34. Py, B., L. Loiseau, and F. Barras. 1999. Assembly of the type II secretion machinery of *Erwinia chrysanthemi*: direct interaction and associated conformational change between OutE, the putative ATP-binding component, and the membrane protein OutL. *J. Mol. Biol.* **289**:659–670.
35. Py, B., L. Loiseau, and F. Barras. 2001. An inner membrane platform in the type II secretion machinery of gram-negative bacteria. *EMBO Rep.* **2**:244–248.
36. Ramer, S. W., G. K. Schoolnik, C.-Y. Wu, J. Hwang, S. A. Schmidt, and D. Bieber. 2002. The type IV pilus assembly complex: biogenic interactions among the bundle-forming pilus proteins of enteropathogenic *Escherichia coli*. *J. Bacteriol.* **184**:3457–3465.
37. Robien, M. A., B. E. Krumm, M. Sandkvist, and W. G. J. Hol. 2003. Crystal structure of the extracellular protein secretion NTPase EpsE of *Vibrio cholerae*. *J. Mol. Biol.* **333**:657–674.
38. Sandkvist, M., L. P. Hough, M. M. Bagdasarian, and M. Bagdasarian. 1999. Direct interaction of the EpsL and EpsM proteins of the general secretion apparatus in *Vibrio cholerae*. *J. Bacteriol.* **181**:3129–3135.
39. Sandkvist, M., J. M. Keith, M. Bagdasarian, and S. P. Howard. 2000. Two regions of EpsL involved in species-specific protein-protein interactions with EpsE and EpsM of the general secretion pathway in *Vibrio cholerae*. *J. Bacteriol.* **182**:742–748.
40. Sandkvist, M., M. Bagdasarian, S. P. Howard, and V. J. DiRita. 1995. Interaction between the autokinase EpsE and EpsL in the cytoplasmic membrane is required for extracellular secretion in *Vibrio cholerae*. *EMBO J.* **14**:1664–1673.
41. Shaw, C. E., and R. K. Taylor. 1990. *Vibrio cholerae* O395 *tcpA* pilin gene sequence and comparison of predicted protein structural features to those of type 4 pilins. *Infect. Immun.* **58**:3042–3049.
42. Shiue, S.-J., K.-M. Kao, W.-M. Leu, L.-Y. Chen, N.-L. Chan, and N.-T. Hu. 2006. XpsE oligomerization triggered by ATP binding, not hydrolysis, leads to its association with XpsL. *EMBO J.* **25**:1426–1435.
43. Sonnhammer, E. L. L., G. Heijne, and A. Krogh. 1998. A hidden Markov model for predicting transmembrane helices in protein sequences. *Proc. Int. Conf. Intell. Syst. Mol. Biol.* **6**:175–182.
44. Strom, M. S., and S. Lory. 1993. Structure-function and biogenesis of the type IV pili. *Annu. Rev. Microbiol.* **47**:565–596.
45. Tacket, C. O., R. K. Taylor, G. Losonsky, Y. Lim, J. P. Nataro, J. B. Kaper, and M. M. Levine. 1998. Investigation of the roles of toxin-coregulated pili and mannose-sensitive hemagglutinin pili in the pathogenesis of *Vibrio cholerae* O139 infection. *Infect. Immun.* **66**:692–695.
46. Taniguchi, T., Y. Akeda, A. Haba, Y. Yasuda, K. Yamamoto, T. Honda, and K. Tochikubo. 2001. Gene cluster for assembly of pilus colonization factor antigen III of enterotoxigenic *Escherichia coli*. *Infect. Immun.* **69**:5864–5873.
47. Taylor, R. K., V. L. Miller, D. B. Furlong, and J. J. Mekalanos. 1987. Use of *phoA* gene fusion to identify a pilus colonization factor coordinately regulated with cholera toxin. *Proc. Natl. Acad. Sci. USA* **84**:2833–2837.
48. Turner, L., J. Lara, D. Nunn, and S. Lory. 1993. Mutations in the consensus ATP-binding sites of XcpR and PilB eliminate extracellular protein secretion and pilus biogenesis in *Pseudomonas aeruginosa*. *J. Bacteriol.* **175**:4962–4969.
49. Waldor, M. K., and J. J. Mekalanos. 1996. Lysogenic conversion by a filamentous phage encoding cholera toxin. *Science* **272**:1910–1914.